euronoise

Active control of engine noise transmitted into cavities: simulation, experimental validation and sound quality assessment

Leopoldo De Oliveira[a], Paul Sas[a], Wim Desmet[b], Karl Janssens[c], Peter Gajdatsy[c] and Herman Van Der Auweraer[c]

[a]KU Leuven, Celestijnenlaan 300B, Departement Werktuigkunde - PMA, 3001 Leuven, Belgium

[b]K.U.Leuven - Dept. of Mechanical Engineering, Celestijnenlaan 300B - bus 2420, 3001 Heverlee, Belgium

[c]LMS International, Interleuvenlaan 68, 3001 Leuven, Belgium

leopoldo.deoliveira@mech.kuleuven.be

Active control has been proposed as a possible solution to cope with low frequency noise reduction in vehicles. Active noise control systems tend to be designed with a target on the sound pressure level reduction. However, the perceived control efficiency for the occupants can be more accurately assessed if psychoacoustic metrics are taken into account. The aim of this paper is to evaluate, numerically and experimentally, the effect of (i) a collocated velocity feedback controller and (ii) an adaptive feedforward controller on the engine sound quality in a vehicle mockup. The simulation scheme is described and experimentally validated. The engine excitation is provided by a sound quality equivalent engine simulator, running on a real-time platform that delivers harmonic excitation in function of the driving condition. The controller performance is evaluated in terms of sound quality metrics such as Roughness, Zwicker- and Specific-Loudness. As a result of the control action, Loudness is significantly reduced while Roughness can either be increased or decreased, depending on the role of the controlled order in the modulation mechanism. Eventually, engine sound quality is improved overall.

1 Introduction

The successful development of new products relies on the capability of assessing the performance of conceptual design alternatives in an early design phase. In recent years, major progress was made hereto, based on the extensive use of virtual prototyping, particularly in the automotive industry. The novelty in this framework is to account for the human perception when defining product performance criteria [1,2].

Additionally, active control has shown the potential to enhance system dynamic performance which allows lighter and improved products. Research done in the last years on smart materials and control concepts has led to practical applications with promising results for the automotive industry [3]. However, to make the step to the design of active sound quality control (ASQC), the control schemes, along with appropriate simulation procedures, need to become an integral part of the product development process [4,5]. In other words, this requires: (i) the product performance metrics to be based on human perception attributes and (ii) the simulation models to support the specific aspects related to smart structures (active systems, actuators, sensors and control logic).

In order to demonstrate the proposed simulation procedure and evaluate the effect of active control on the perceived sound quality (SQ), a vibro-acoustic cabin mock-up is selected (Fig.1). It consists of a simplified car cavity with rigid acoustic boundary conditions. The passenger compartment (PC) and the engine compartment (EC) are connected through a flexible firewall which allows noise generated in the EC to be transmitted to the PC. A sound source placed in the EC works as a primary disturbance source. The primary source is driven by a real-time engine simulator, capable of delivering a harmonic excitation based on the engine orders' amplitude and phase [6]. Two control strategies have been evaluated: (i) an ASAC scheme involving a collocated velocity feedback controller with a structural sensor/actuator pair (SAP) and (ii) an adaptive feedforward controller with a structural secondary actuator and an acoustic error sensor.

The control strategies are presented in Section 2. In Section 3, the simulation procedure is described. The experimental validation and the results obtained with both controllers, in terms of Roughness [7], Specific-Loudness and Zwicker-Loudness [8,9] are treated in Section 4. Finally, some general conclusions are addressed in Section 5.

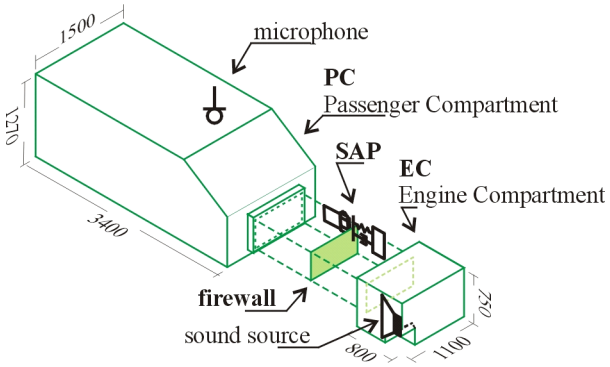

Figure 1 – Vehicle mock-up

2 Control Strategies

As mentioned before, two distinct control strategies are considered in this paper, a collocated velocity feedback and an adaptive feedforward control.

The collocated velocity feedback consists of a linear time invariant controller based on structural sensors and actuators, tuned according to the acoustic pressure measured on the PC. This controller acts like an active damper by introducing a force proportional to the measured velocity signal (Fig.2). This method is suitable for broadband disturbance and is, theoretically, inherently stable. The use of a digital integrator requires a high-pass filter to avoid drift.

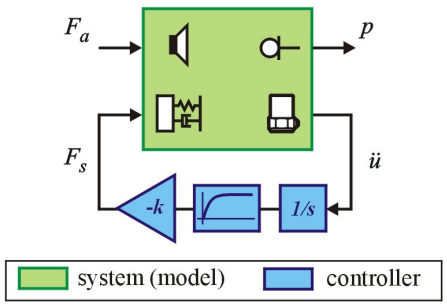

Figure 2 – Feedback control

The adaptive feedforward strategy is based on a modified version of the Fx-LMS [10]. This scheme was proposed to increase the convergence speed of the standard Fx-LMS, which is achieved by compensating for the secondary path dynamics. As it can be seen in Fig.3, the error signal used for the LMS update is the signal coming from the error microphone diminished by the estimate of the secondary

path contribution ($F_s \times \hat{\mathbf{S}}$). In this way, the Fx-LMS behaves closer to a purely LMS algorithm.

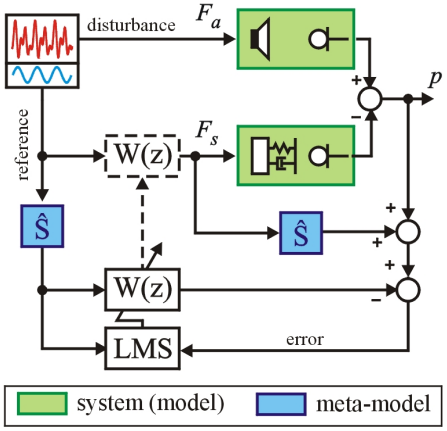

Figure 3 – Adaptive feedforward control

3 ASAC simulation scheme

The modeling procedure presented here is a general framework in which different control strategies can be implemented, revealing the functionality of such an approach to the assessment of conceptual design performance [1,5,11].

One of the key aspects in this modeling approach resides in deriving reasonably sized models that integrate the structural and acoustic components along with the control algorithm. In order to fulfill this requirement, a fully coupled finite element (FE) model of the vibro-acoustic system is written as a modal state-space (SS) model (Eq.1). As a result of using the coupled vibro-acoustic modal base, any combination of structural and acoustic inputs/outputs can be used for the control design, e.g., an acoustic source in the EC, structural sensors and actuators on the firewall and microphones on the PC.

$$\begin{Bmatrix} \dot{\mathbf{q}} \\ \ddot{\mathbf{q}} \end{Bmatrix} = \begin{bmatrix} \mathbf{0} & \mathbf{I} \\ -\mathbf{\Omega}^2 & -\mathbf{\Gamma} \end{bmatrix} \begin{Bmatrix} \mathbf{q} \\ \dot{\mathbf{q}} \end{Bmatrix} + \begin{bmatrix} \mathbf{0} \\ \mathbf{\Phi}_L^T \mathbf{B} \end{bmatrix} \begin{Bmatrix} \mathbf{F}_s \\ \mathbf{F}_a \end{Bmatrix} \quad (1)$$

$$\begin{Bmatrix} \mathbf{u} \\ \mathbf{p} \end{Bmatrix} = \begin{bmatrix} \mathbf{C}\mathbf{\Phi}_R & \mathbf{0} \end{bmatrix} \begin{Bmatrix} \mathbf{q} \\ \dot{\mathbf{q}} \end{Bmatrix} \quad (2)$$

where $\mathbf{q}$ is the vector of modal amplitudes of the Eulerian vibro-acoustic model in displacement $\mathbf{u}$ and pressure $\mathbf{p}$; $\mathbf{B}$ and $\mathbf{C}$ are Boolean matrices that select input and output DoFs, respectively; $\mathbf{F}$ is the load vector, $\mathbf{\Phi}_L$ and $\mathbf{\Phi}_R$ are the left and right-eigenvector which hold the following properties:

$$\mathbf{\Phi}_L^T \begin{bmatrix} \mathbf{M}_s & \mathbf{0} \\ \rho_o \mathbf{K}_c^T & \mathbf{M}_a \end{bmatrix} \mathbf{\Phi}_R = \mathbf{I} \quad (3)$$

$$\mathbf{\Phi}_L^T \begin{bmatrix} \mathbf{K}_s & \rho \mathbf{K}_c \\ \mathbf{0} & \mathbf{K}_a \end{bmatrix} \mathbf{\Phi}_R = \mathbf{\Omega}^2 \quad (4)$$

$$\mathbf{\Phi}_L^T \begin{bmatrix} \mathbf{D}_s & \mathbf{0} \\ \mathbf{0} & \mathbf{D}_a \end{bmatrix} \mathbf{\Phi}_R = \mathbf{\Gamma} \quad (5)$$

where ρ_O is the air density, the index a refers to acoustic and s to structural DoFs, $\mathbf{K}$, $\mathbf{D}$ and $\mathbf{M}$ are the stiffness, damping and mass matrices, respectively, and $\mathbf{K}_c$ is the vibro-acoustic coupling matrix; $\mathbf{I}$ is the identity matrix, $\mathbf{\Omega}$ is the matrix of natural frequencies and $\mathbf{\Gamma}$ is the modal damping matrix. For a more detailed description of the state-space model, the reader is referred to [11].

The original FE model, consisting of the firewall and the cavities, contains 24192 DoFs (23196 unconstrained acoustic and 1026 unconstrained structural). Applying the aforementioned modal reduction, it has been reduced to a SS model with $2 \times N$ DoFs, related to the N kept modes, with force and volume velocity as inputs and displacement and pressure as outputs. The modal base was built with modes ranging from 0 to 400Hz, resulting in $N = 107$.

The numerical validity of the reduced model is illustrated by comparing FRFs from the original FE model with the reduced SS model (Fig.2). The system inputs are volume velocity applied in the EC (acoustic input) and force applied on the firewall (structural input); and the outputs are pressure measured in the PC (acoustic output) and displacement measured on the firewall (structural output). The good correlation between the SS and the FE model validates the model reduction procedure.

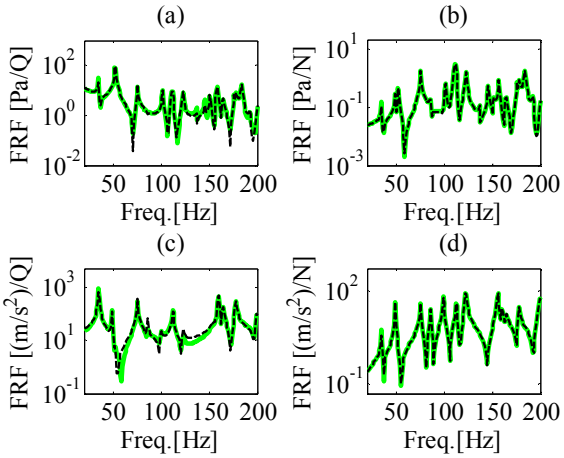

Figure 4 - Comparison between (▪▪▪) FE and (▬) SS FRFs: (a) Acoustic/Acoustic, (b) Acoustic/Structural, (c) Structural/Acoustic and (d) Structural/Structural

For the adaptive feedforward simulations, a meta-model is needed to represent $\hat{\mathbf{S}}$ as a FIR filter. As depicted in Fig.4, this meta-model can be obtained with an LMS-based off-line secondary path estimation [12]. After convergence, **W(z)** should resemble the secondary path transfer function.

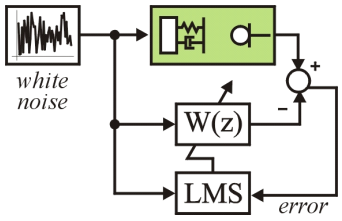

Figure 5 – Off-line secondary path estimation

4 Experimental Validation

In Figure 6, the FRFs derived from the reduced SS model are compared with the FRFs measured on the cabin mock-

up. These FRFs include the transfer paths to the driver's microphone from both inputs: primary acoustic source and secondary structural actuator. The vibro-acoustic system has been excited with white noise. The FRFs are measured with an Hv estimator, while input and output signals are filtered with Hanning windows.

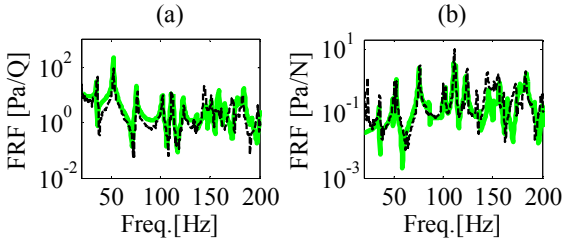

Figure 6 – Comparison of (▪▪▪) experimental and (▬) numerical FRFs: (a) acoustic input and (b) structural input

For the adaptive controller, the reference for the FRFs should be the voltage signal sent to either the shaker (V_S) or the acoustic source (V_P). Fig.7 shows a comparison of such FRFs and the Fourier transform of the FIR filters identified as in Fig.5.

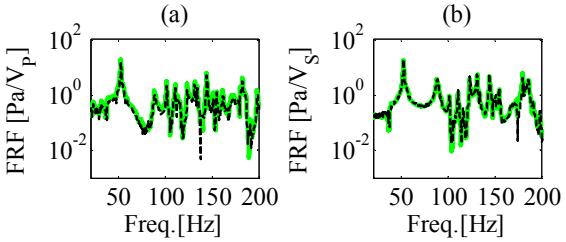

Figure 7 – Comparison of (▪▪▪) FRFs and (▬) FFT of identified FIR filters: (a) primary and (b) secondary paths

In both cases (Figs.6 and 7) comparisons present a good agreement. Few discrepancies arise, a.o., from the lack of accuracy in determining the exact place of the disturbance source, sensor/actuator pair and microphones and from assuming the disturbance source as an ideal point source. Such mismatches are expected and believed not to harm the accuracy of the results, as previous analyses have shown [1,5,11].

Moreover, in order to have an engine-like excitation, which allows meaningful SQ measurements, a real-time engine simulator was used [6]. SQ-equivalent engine models are used in product development, as it enables one to experience and assess the NVH of a virtual (or real) vehicle under various driving conditions [6,13]. The novelty here is the use of such device as a source of excitation. In this case, the engine sound, which is a function of the driving condition (engine speed, gear, throttle and brake positions, etc.) is fed to the acoustic source in the EC. Results obtained as such, benefit from this SQ-equivalence and, therefore, allow the correlation with real engine sounds.

Henceforth, two driving conditions are analyzed, namely 50km/h (1634rpm) and 80km/h (2694rpm). The excitation consists of 20 complex orders (0.5, 1.0, 1.5, …, 10), from which the amplitudes are depicted in Fig.8.

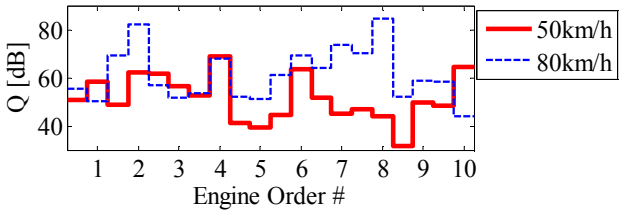

Figure 8 – Order amplitudes for two driving conditions

The measured excitation can be used as disturbance input in the simulations to obtain the passive and active responses that can be compared to the measured ones. Due to the SQ equivalence of the excitation, SQ metrics can be calculated from the resulting pressure signals, from which rather general conclusions can be drawn.

4.1 Feedback control

For the feedback controller setup, the feedback gain k (Fig.2) is optimized to minimize the sound pressure level measured at the driver's head position [11]. The order amplitudes for the passive and active system can be seen in Fig.9. As it can be seen, some orders are damped and some slightly amplified. Overall, the sound pressure level (SPL) is reduced by 7dB.

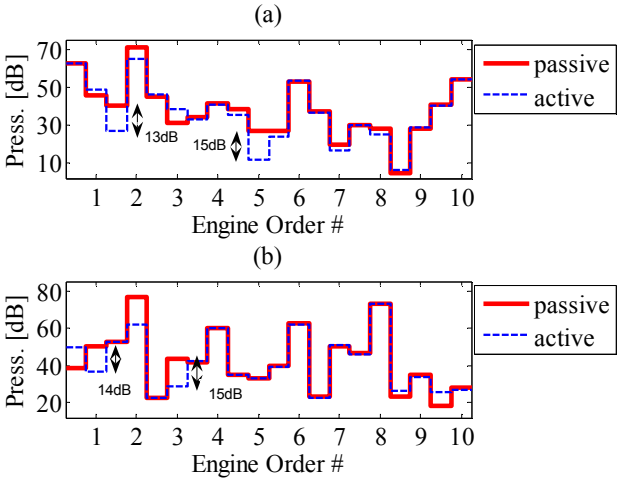

Figure 9 - Order amplitudes for feedback control and two driving conditions, (a) 50km/h and (b) 80 km/h

Figure 10 shows comparisons of the passive and active Specific Loudness perceived by the driver for 50km/h and 80km/h driving conditions. The corresponding Zwicker Loudness is presented in Table 1. In this way it is possible to affirm that the reduction in SPL can be clearly perceived by the occupants.

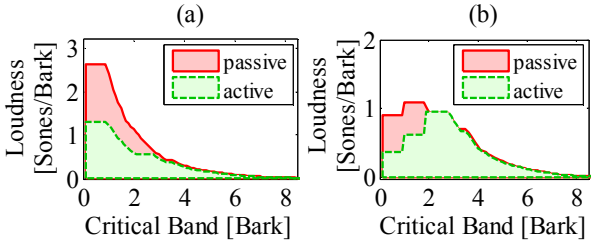

Figure 10 – Specific Loudness
(a) @ 50km/h and (b) @ 80km/h

Table 1 - Zwicker Loudness [Sones]

	experimental		simulated	
	50km/h	**80km/h**	**50km/h**	**80km/h**
passive	5.9	4.2	6.1	4.1
active	3.4	2.3	3.3	1.8

As a result of the feedback control, Roughness can be slightly increased. This is due to the attenuation of some order amplitudes, which can unmask orders in their vicinities, allowing modulation and, therefore, increasing roughness. Previous simulation results [1] show that this feedback controller increases Roughness in some regions, though not affecting the maximum Roughness value.

Table 2 presents the values obtained for both driving conditions. In general, Roughness at the driver's head position is increased, but still remains quite bellow the maximum value encountered in the cavity. In fact the values are rather low, which indicates that Roughness should not be of much concern to the interior SQ at those driving conditions.

Table 2 – Roughness at the driver's head position [Asper]

	passive	**active**
50km/h	4.8×10^{-3}	2.5×10^{-2}
80km/h	2.5×10^{-2}	3.6×10^{-2}

4.2 Adaptive feedforward control

To implement the adaptive feedforward control, the FIR filter $\hat{\mathbf{S}}$ is estimated as depicted in Fig.5. The frequency sample for the real-time DSP is 2kHz. The frequency of 10th order at 80km/h is 450Hz, well below the DSP Nyquist frequency.

The reference signal consists of a sine wave with the same frequency of the targeted order, which yields an adaptive notch-filter [12]. This is an interesting feature for the intended future application of such controllers, i.e., order balancing. In order to independently tune different orders' amplitudes, similar controllers could be connected in parallel since each narrowband action would not interfere with each other. Also, due to the narrow band of the control action, it is affordable to use a short filter **W(z)**, in this case a order-10 FIR filter.

Figure 11 shows the 2nd order cuts for the passive, standard Fx-LMS and modified Fx-LMS. These simulation results show that the modified Fx-LMS considerably increases the convergence speed. After 500 iterations (.25s @ 2kHz frequency sample) the modified Fx-LMS has reduced 15dB while the standard algorithm only 5dB.

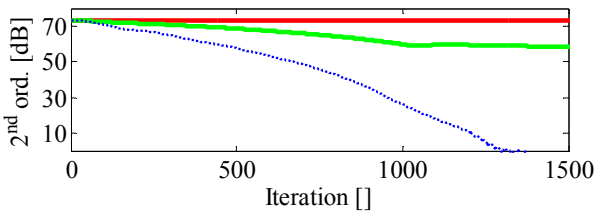

Figure 11 – 2nd order cuts for (▬) passive, (▬) standard Fx-LMS and (▪▪▪) modified Fx-LMS.

Figure 12 shows the experimental order amplitudes measured by the driver's microphone with controller on and off for both driving conditions. The 2nd order is targeted in both cases and the reduction obtained specifically for this order is 34dB for 50km/h and 51dB for 80km/h.

When it comes to the SQ analysis, some discrepancies between the results for feedback and feedforward should be stressed. The feedback measurements have a slightly lower frequency range. Although comparisons for 50km/h can be done, results related to 80km/h should be analyzed separately for each control strategy.

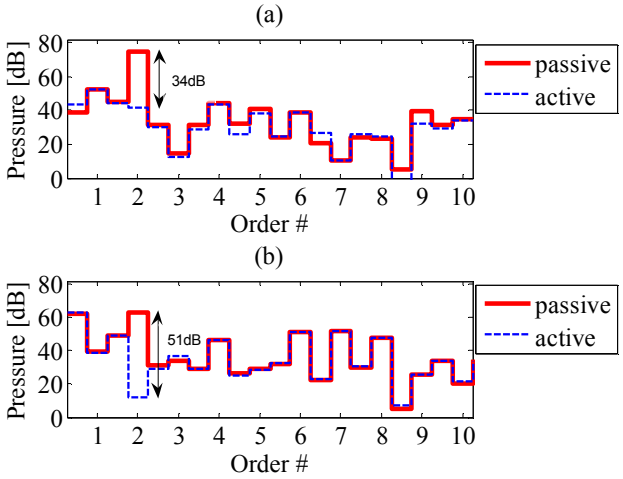

Figure 12 – Order amplitudes for feedforward control and two driving conditions, (a) 50km/h and (b) 80 km/h

The Specific Loudness plots for 50km/h and 80km/h are shown in Fig.13. As it can be seen, even if the controller is targeting just a single order, the effect on the perceived loudness is quite noticeable. The Zwicker Loudness for passive and active systems (Table 3) reveals a reduction of 45% in the perceived volume.

Table 3 - Zwicker Loudness [Sones]

	50km/h	**80km/h**
passive	6.1	7.5
active	1.9	5.8

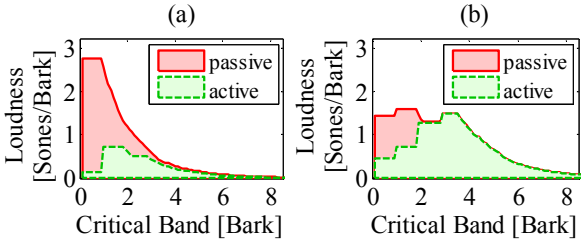

Figure 13 – Specific Loudness
(a) @ 50km/h and (b) @ 80km/h

Table 4 – Roughness at the driver's head position [Asper]

	passive	**Active**
50km/h	3.4×10^{-3}	2.3×10^{-2}
80km/h	3.3×10^{-2}	1.7×10^{-2}

When reducing the amplitude of an order, Roughness can be affected in two ways: (i) if that is a dominant order, by reducing it, modulating orders can be unmasked and Roughness increases, or (ii) if that is one of the modulating orders, Roughness is decreased. At 50km/h, there is booming of the second order, such that the controller gives rise to Roughness (Table 4). On the other hand, at 80km/h, the second order contributes to the modulation, hence Roughness is reduced.

5 Conclusions and Future Work

This paper describes a modeling procedure for ASAC, which allows the use of standard vibro-acoustic FE models in the control design. The modeling procedure is experimentally validated with a vehicle mock-up.

The proposed experimental setup is acoustically excited by a SQ-equivalent engine simulator, typically employed in auralization. The use of such scheme allows repeatable measurements with engine-like excitation signals, furnishing results that can be directly correlated to automotive applications.

The results for Loudness attenuation are presented in terms of Specific and Zwicker Loudness, the latter being linearly related to the human sensation of volume. The results indicate that the controllers are quite effective with respect to the occupants perception of the sound field. While the feedback control provides an efficient broadband reduction that could be targeted to road or wind-noise, independent order control (with varying rpm) can only be achieved by an adaptive scheme. The presented adaptive feedforward control converges fast which indicates it could cope with varying rpm within the transient regime, though such conditions have not yet been evaluated.

While Loudness is always improved, the only way to improve Roughness is through order balancing. The only control strategy presented here which is capable of coping with this is the adaptive feedforward. In that way, the desired order profiles (amplitude and phase vs. rpm) can be defined with the aid of SQ-equivalent models and further used to define target values for the feedforward controller.

A next step in this study will investigate more efficient convergence algorithms in order to cope with fast varying engine speeds. Also, the inclusion of such adaptive feedforward controllers in the real-time engine simulator is under study, towards a fully numerical ASQC design platform.

Acknowledgements

The research of Leopoldo P. R. de Oliveira is supported in the framework of a bilateral agreement between KU Leuven and University of São Paulo. The research presented in this paper was performed as part of the Marie Curie RTN project: A Computer Aided Engineering Approach for Smart Structures Design (MC-RTN-2006-035559).

References

[1] L.P.R. de Oliveira, *et al.*, Active sound quality control of engine induced cavity noise, Mechanical Systems and Signal Processing (2008), doi:10.1016/j.ymssp.2008.04.005

[2] D. Berckmans, *et al.*, Model based synthesis of aircraft noise to quantify human perception of sound quality and annoyance, Journal of Sound and Vibration 311 (2008) 1175-1195.

[3] S. Hurlebaus, L. Gaul, Smart structure dynamics, Mechanical Systems and Signal Processing, 20 (2006) 255-281.

[4] S.M. Kuo, A. Gupta, S. Mallu, Development of adaptive algorithm for active sound quality control, Journal of Sound and Vibration, 299 (2007) 12-21.

[5] H. Van der Auweraer, *et al.*, Virtual prototyping for sound quality design of automobiles, Sound and Vibration, April (2007) 26-30.

[6] K. Janssens, P. Van de Ponseele, M. Adams, The integration of sound quality equivalent models in a real-time virtual car sound environment. Proceedings of DAGA Conference, 18-20 March, 2003, Aachen, Germany, 6p.

[7] K. Janssens, *et al.*, An On-line Order-based Roughness Algorithm, SAE Noise and Vibration Conference, 2007, USA, SAE Paper No. 07NVC-173.

[8] E. Zwicker, H. Fastl, Psychoacoustics: Facts and Models, Srpinger Series in Information Sciences, Heidelberg, 1999, Ed.2.

[9] International Organization for Standardization, Method for Calculating Loudness Level, ISO-532B, 1975.

[10] C. Bao, Adaptive algorithms for active noise control and their applications, PhD Thesis, Katholieke Universiteit Leuven, Mechanical Engineering Department – PMA, 1994.

[11] L.P.R. de Oliveira, *et al.*, Concurrent mechatronic design approach for active control of cavity noise, Journal of Sound and Vibration (2008), doi:10.1016/j.jsv.2008.01.009

[12] S.M Kuo, D.R. Morgan, Active Noise Control Systems: Algorithms and DSP implementation, John Wiley and Sons, Inc. – New York (1996).

[13] R. Williams, *et al.*, Using an interactive NVH simulator to compute and understand costumer opinions about vehicle sound quality, Simposium on International Automotive Technology, 2007, Pune, India, SAE Paper No. 2007-26-036.